



**HAL**  
open science

## **Three-dimensional characterization of cortical bone microstructure by microcomputed tomography: validation with ultrasonic and microscopic measurements**

Armelle Basillais, Sabine F Bensamoun, Christine Chappard, Barbara Brunet-Imbault, Gérald Lemineur, Brice Ilharreborde, Marie-Christine Ho Ba Tho, Claude-Laurent Benhamou

### ► To cite this version:

Armelle Basillais, Sabine F Bensamoun, Christine Chappard, Barbara Brunet-Imbault, Gérald Lemineur, et al.. Three-dimensional characterization of cortical bone microstructure by microcomputed tomography: validation with ultrasonic and microscopic measurements. *Journal of Orthopaedic Science*, 2007, 12 (2), pp.141-148. 10.1007/s00776-006-1104-z . hal-03812662

**HAL Id: hal-03812662**

**<https://hal.science/hal-03812662>**

Submitted on 15 Oct 2022

**HAL** is a multi-disciplinary open access archive for the deposit and dissemination of scientific research documents, whether they are published or not. The documents may come from teaching and research institutions in France or abroad, or from public or private research centers.

L'archive ouverte pluridisciplinaire **HAL**, est destinée au dépôt et à la diffusion de documents scientifiques de niveau recherche, publiés ou non, émanant des établissements d'enseignement et de recherche français ou étrangers, des laboratoires publics ou privés.

**Three dimensional characterization of cortical bone microstructure by micro-computed tomography : validation with ultrasound and microscopic measurements**

A. Basillais,<sup>1</sup> S. Bensamoun,<sup>2</sup> C. Chappard,<sup>1</sup> B. Brunet-Imbault,<sup>1</sup> G. Lemineur,<sup>3</sup> B. Ilharreborde,<sup>4</sup> M.C. Ho Ba Tho,<sup>2</sup> C.L. Benhamou<sup>1</sup>

<sup>1</sup> INSERM U658, CHR d'Orléans, Hôpital Porte Madeleine BP 2439 45032 Orléans Cedex 1, France

<sup>2</sup> Laboratoire de Biomécanique et Génie Biomédical, CNRS-UMR6600, Université de Technologie de Compiègne, BP 20529, 60205 Compiègne Cedex, France

<sup>3</sup> Laboratoire d'Electronique, Signaux, Images, Polytech' Orléans, BP 6744 45067 Orléans Cedex 2, France

<sup>4</sup> Département de chirurgie orthopédique pédiatrique, Hôpital Robert Debré, 75935 Paris Cedex 19, France

Running title : Human cortical bone analysed with  $\mu$ CT

Corresponding author:

A. Basillais

INSERM U658, CHR d'Orléans, Hôpital Porte Madeleine BP 2439 45032 Orléans Cedex 1, France

Tel : 00 33 (0)2.38.74.40.61

Fax : 00 33 (0)2.38.74.40.24

armelle.basillais@chr-orleans.fr

## **ABSTRACT**

**Background.** The porosity of human cortical bone is one of the major parameters conditioning bone strength. The purpose of this study was to validate the characterization of human cortical bone microarchitecture using microcomputed tomography ( $\mu$ CT). To validate this  $\mu$ CT technique, the structural measurements were compared with other techniques such as ultrasound and Scanning Electron Microscopy.

**Methods.** Nineteen cortical samples were extracted from the superior, middle and inferior shaft of three human femurs (FI, FII, FIII). The samples were scanned by a  $\mu$ CT with an isotropic resolution of 8  $\mu$ m. Most of the structural parameters used for trabecular microarchitecture were calculated in order to characterize the network of pores. On the same cortical samples, 1) ultrasound measurements were performed, using contact transmission emitter-receptor, to determine elastic coefficient and Young modulus 2) Scanning Electron Microscopy was made on femoral cross sections from FII to evaluate the porosity.

**Results.** The morphological parameters showed a wide range of variation depending of the level in diaphysis. Porosity measured by  $\mu$ CT was significantly correlated with porosity measured by SEM ( $r=0.91$ ,  $p<0.05$ ). Moreover, all the morphological parameters showed high correlation coefficients with elastic coefficient and Young modulus leading to a validation of our 3D analysis.

**Conclusions.** The strong correlations between the structural and mechanical properties obtained with the three different techniques allow to validate the  $\mu$ CT technique used to characterize the cortical bone microstructure. Porosity measurement might be of importance for the clinicians and researchers to get a better understanding and evaluation of bone fracture in elderly patients.

## INTRODUCTION

Micro-computed tomography ( $\mu$ CT) has been widely used to characterize trabecular bone structure and the most common application is the study of trabecular bone alterations<sup>1-5</sup>. Nevertheless, cortical bone globally represents 80 % of the skeleton bone mass<sup>6</sup> and therefore contributes to the mechanical bone strength. The cortical bone porosity is one of the major determinants of bone strength : age-related increase in cortical porosity accounted for 76 per cent of the bone strength loss in proximal femur<sup>7</sup>. A better understanding of the relationships between cortical bone microstructure and bone strength might be relevant for the evaluation of fracture risk. Human cortical bone is arranged as a compact structure, including a network of pores : Havers / Volkmann canals on one hand, resorption spaces on the other hand. The assessment of cortical bone properties is now possible since the spatial resolution of  $\mu$ CT system has been improved.  $\mu$ CT may provide a three dimensional (3D) analysis with a measurement of parameters which describe quantitatively the microstructure of the cortical bone.

Thresholding algorithms are applied to binarize images in order to separate bone from background. Usually for the trabecular analysis we are interested by pixels corresponding to bone. On the contrary in cortical bone, we are interested in characterizing the void part of a compact structure. Therefore, calculations have to be done on the voids and consequently the algorithms have to be adapted. This fit may be obtained by inverting the 3D images then considering the pores as a “pseudo trabecular” structure and the solid part as a “pseudo medullar” structure. In this case, most of parameters obtained in cancellous bone can be applied to describe cortical porosity<sup>8</sup>. Studies of cortical bone are usually processed by techniques derived from histomorphometry which provide a two dimensional (2D) analysis<sup>9-13</sup>. These studies evaluate the percentage of total intracortical porosity and the correlation with parameters like Bone Mineral Density (BMD)<sup>9</sup> or age<sup>11-13</sup>. There was a

negative coefficient correlation between porosity and BMD<sup>9</sup>. The cortical porosity was shown to increase with age<sup>11-13</sup>. The cortical porosity was also increased in post menopausal women comparatively with premenopausal women<sup>14</sup>.

The relationship between cortical porosity and mechanical properties has been characterized by few authors<sup>9,10</sup>. Bousson et al.<sup>15</sup> reported the relationship between cortical BMD assessed by CT technique and the intracortical porosity derived on microradiography. Recently, Cooper et al.<sup>16</sup> validated the use of 2D  $\mu$ CT sections of 100  $\mu$ m thickness to measure porosity and related parameters (mean pore area and pore density). They compared these parameters with classical microradiographic measurements on 100  $\mu$ m slices. Only a few papers were dedicated to 3D analysis of cortical bone porosity. Wachter et al.<sup>17</sup> have studied the interest of  $\mu$ CT imaging to assess quantitatively cortical bone porosity by comparison with histomorphometric measurements. The parameters describing osteon and haversian canal dimensions by histomorphometry were not correlated with  $\mu$ CT porosity<sup>17</sup>. The authors interpreted these results in relation to a low resolution of the  $\mu$ CT acquisition. Recently, a 3D approach has been reported by Stout et al.<sup>18</sup> from mathematical 3D reconstruction of 34 serial histological bone sections. However, histomorphometric studies have the main drawbacks to be destructive and subject to deformation artefacts<sup>18,19</sup>. Three dimensional methods offer a structural complement of information to histomorphometric techniques as demonstrated by Cooper et al.<sup>8</sup> who pointed out that  $\mu$ CT could be an useful tool to perform the 3D analysis of cortical bone. Bousson et al.<sup>19</sup> have worked on synchrotron  $\mu$ CT images, with a 15.76  $\mu$ m resolution, on the femoral neck cortex. They have demonstrated the ability to describe the arrangement of the osteonal system. They evaluated the intracortical porosity and the pore diameter, and suggested the potential of measuring microarchitecture parameters comparable to the trabecular microarchitecture parameters. They also underlined the interest to validate this analysis, for instance versus 2D histological images<sup>19</sup>.

The purpose of the present study was to investigate the microarchitecture of the human femoral cortical bone by 3D analysis on  $\mu$ CT images. We have characterized cortical bone morphological parameters such as pore number, pore diameter, pore surface, degree of anisotropy and topological parameter such as the fractal dimension. A strong correlation was established between the 3D morphological analyses and 1) the porosity parameters measured with the scanning electron microscopy (SEM) and 2) the mechanical parameters measured with the ultrasound technique. Measuring cortical porosity would be of interest to improve the clinical assessment of bone quality and evaluate in further study the risk of fracture in elderly patients.

## MATERIAL AND METHODS

### *Specimens*

Three cadaveric femurs (FI, FII, FIII) (male, mean age of  $70 \pm 6$ ) were obtained from the anatomical laboratory of Hospital University of Amiens. Nineteen samples of cortical bone were cut transversally with a low-speed diamond saw (MICROCUT 2, Hergon, Argenteuil, France) in the lateral and medial sides of the three shafts. Four cubic samples (5x5x5mm) were cut in the superior shaft (Fig. 1 level A) of the first femur (FI). For the second femur (FII), 10 parallelepiped samples (5x4x13mm) were cut on a 10cm length in the middle and inferior shaft (levels B and C Fig. 1). For the last one (FIII), 5 parallelepiped samples (5x4x13mm) were cut on a 5.5cm length in the distal shaft (level C Fig. 1). Each sample was ground with sandpaper (grit #1200) and then polished with 0.5 $\mu$ m aluminum powder.

From the femur II level B, three cross sections were cut between 40 and 70 % of the total length of the femur. The average of the thickness section was about 1.99 (SD 0.002) mm measured by a digital micrometer (Mitutoyo, 293, Tokyo, Japan). The details of the measurements are given elsewhere<sup>20</sup>.

### *Image acquisition : microcomputed tomography ( $\mu$ CT)*

All the samples were scanned by using a Skyscan ® 1072  $\mu$ CT. This device used a micro X-Ray source (20-80kV, 100 $\mu$ A, filtered with a 1mm thick aluminium filter). The transmitted X-Ray beam was recorded by a scintillator coupled to a 1024x1024 pixels 12-bits digital cooled CCD camera. The radiographic projections were acquired at 80kV, 100  $\mu$ A with a fixed exposure time of 3 seconds per frame and two frames averaging to improve signal to noise

ratio. Transmission X-ray images were acquired with a rotation step of  $0.9^\circ$  leading to 200 views over 180 degrees-of rotation. The voxel size was isotropic and fixed at  $8\ \mu\text{m}$ . After scanning, 900 slices were reconstructed with the manufacturer reconstruction software based on Feldkamp algorithm.

### *Image processing*

For each femur, the largest volume of interest as possible was selected corresponding to 7 mm length (femur II and III) and 3 mm length (femur I). The volumes were binarized using a different threshold for each femur. This value corresponded to the middle between the peak corresponding to cortical bone and the peak corresponding to cavities (Fig. 2).

### *Image analysis*

Morphological parameters were measured by making the analogy between the parameters which characterize trabecular structure and those which can describe cortical porosity. In order to characterize porosity, calculations were done in pixels attributed to voids. After thresholding, binarization led to a separation of porosity and matter. Morphological parameters were derived by using Skyscan software CTan®. The cortical porosity (pore volume on total sample volume  $PoV/TV$ ) was measured. The distribution of pore diameter ( $PoDm$ ,  $\mu\text{m}$ ) and spacing ( $PoSp$ ,  $\mu\text{m}$ ) was calculated using the method of the spheres described by Hildebrand and Ruegsegger<sup>21</sup> which is model independent. The pore number ( $PoN$ ,  $\text{mm}^{-1}$ ) was defined as the inverse of the mean distance between the middle axes of the structure<sup>22</sup>. These axes were identified by a skeletonisation process. The pore surface ( $PoS$ ,  $\text{mm}^{-2}$ ) was obtained by triangulation. Description of the architecture was attended with the degree of anisotropy (DA). Mean Intercept Length and Eigen analysis were used to calculate  $DA$ <sup>23</sup>.  $DA$  equals 1 for a perfect isotropic structure. The highest is  $DA$ , the more anisotropic is the structure.

Fractal dimension was obtained with a box counting algorithm<sup>24,25</sup>. It was applied to the binarized volumes using the same threshold than for the structural analysis described above. A grid consisting of box size  $\epsilon$  was superimposed on the cortical structure. The size of boxes has been ranged from 2 to 256 pixels. For a given size of box side  $\epsilon$ , the number of boxes  $N(\epsilon)$  containing the boundary of the bone were determined. The box size  $\epsilon$  versus the number of boxes  $N(\epsilon)$  was plotted on log-log graphs. From the linear portion of this curve, the fractal dimension was defined to be the negative slope of the curve.

#### *Determination of porosity derived from Scanning Electron Microscope images*

Backscattered environmental scanning electron micrographs (XL 30 ESEM-FEG) were produced under high vacuum at 20 kV with a magnification of 22. Uncompressed Tiff images size were obtained with mean resolution of 5  $\mu\text{m}$  per pixel. A total of 40 images were obtained for each section. Regions of interest (square of 3 mm) were defined on each section of the femur II, in relation with the localization of the parallelepipedic samples used for  $\mu\text{CT}$  acquisitions. The regions of interest were transferred into a custom made software<sup>26</sup> in order to perform an edge detection of the pores. The cross section areas of the pores were calculated with Patran V.9 software (MCS. Software). The porosity expressed in percent was defined by the ratio between the total area of the pores<sup>20</sup> divided by the total section of interest.

#### *Transmission ultrasonic technique*

An ultrasonic transmission technique (Fig. 3) was used<sup>27</sup> to determine acoustic velocities on cortical bone tissues. The cortical samples were disposed between a couple of contact transducers used at low (Panametrics V1011RB, 75KHz) and high (Panametrics V106RB, 2.25MHz) frequencies. The generator (HP 3312A) sent impulsions, which were received by the first transducer acting as a transmitter. Then the wave is propagated through the sample and the second transducer receives the longitudinal waves, which was visualized on an

oscilloscope (Tektronics TDS 3032). The ratio length of the sample and the time of propagation enable to measure the wave velocities. Different types of wave propagation were investigated on the same sample: bar and bulk waves. These types of propagation depend on the ratio between the wavelength ( $\lambda$ ) and the transversal dimension (D) of the samples: at high (2.25MHz) frequency  $\lambda \lll D$  and at low (75KHz) frequency  $\lambda \ggg D$ . The relation between the different velocities and the mechanical properties are respectively:

$$V_{ij}^{bar} = \sqrt{\frac{E_{ij}}{\rho}} \quad V_{ij}^{bulk} = \sqrt{\frac{C_{ij}}{\rho}}$$

$\rho$  is the density ( $\text{kg/m}^3$ ),  $E_{33}$  the Young moduli (Pa) and  $C_{33}$  the elastic coefficient (Pa) of the material, i being the direction of the wave propagation and j corresponding to the movement of the particles<sup>28</sup>. In the present study the longitudinal waves were measured in the axial direction of the material,  $V_{ij} = V_{33}$ .

The calibration of the ultrasonic transmission technique was performed with different metal samples (copper, stainless steel, Plexiglass, PVC) with a size of 5x5mm and 5x10mm. The range of velocities for these materials measured at 75 KHz and 2.25 MHz varied between 845m/s and 5674m/s. The longitudinal velocity of cortical bone (about 3500m/s at low frequency and 4000m/s at high frequency) is included in the range of the theoretical velocities of these materials.

### *Statistical analysis*

Statistical analyses were done using NCSS software (Kaysville, USA). Spearman correlation coefficients were used to correlate the microstructural parameters with the mechanical properties. Simple linear regression was used to examine the relationship between 2D porosity assessed by SEM and 3D porosity assessed by  $\mu\text{CT}$ . A stepwise regression was calculated to

determine the morphological parameters explaining the porosity after checking the lack of outliers.

## RESULTS

### *3D Visualization*

The 3D representation of cortical bone (Fig. 4) points out the different types of porosity present in cortical bone: small vertical canals which can be attributed to Havers canals, larger canals which correspond to resorption spaces. On a small region of interest, it was possible to differentiate the Havers and Volkman canals in the structure (Fig. 5) and to see the interconnections between the canals.

### *Porosity and Structural parameters*

Table 1 gives all the mean values of the morphological and topological parameters measured with  $\mu$ CT for the three femurs as a function of the level of sampling on the diaphysis.

Significant correlation was found between porosity measured on femoral cross sections (FII) by Scanning Electron Microscopy and porosity measured by  $\mu$ CT ( $r = 0.91$ ,  $p < 0.05$ ) for the samples of the femur II ( $n = 6$ ).

Multiple stepwise regressions were performed on porosity with combination of the various morphological and topological parameters and results are summarized in Table 2. Morphological characterization of the porosity (size and number of the pores) explained most of the porosity variance. Pore number remained the primary determinant of porosity ( $r^2 = 0.80$ ,  $p < 10^{-4}$ ). The pore diameter contributed significantly to global porosity as it explained 16 % of the variance ( $p < 10^{-4}$ ). Finally, with a combination of the two parameters describing in details the pores, 96 % of the variance of the porosity remained explained (Table 2).

Table 3 gives the Spearman correlation coefficients between mechanical results and morphological parameters. For all microstructural (PoV/TV, PoS/PoV, PoDm, PoSp and PoN) and topological (FD, DA) parameters, a significant correlation with ultrasonic

parameters was observed. Multivariable regression analysis was not feasible since the distribution of the elastic coefficient was not normal.

## DISCUSSION

These data confirm that  $\mu$ CT may be an efficient tool to characterize the cortical microstructure of human bone *in vitro*. To our knowledge, this is the first study reporting topological and anisotropy parameters of cortical bone. A good degree of validation was obtained by comparison with mechanical properties, and with 2D porosity evaluated on SEM images.

Being a highly compact material, cortical bone does not appear as a good candidate for 3D analysis if we focus on the characterization of the compact bone itself. Nevertheless, the analysis becomes possible when the calculations are not carried out on the matter, but on the pores. In this configuration, the algorithms developed for trabecular bone which are not based on a structural model are suitable to characterize cortical pores. Some evaluations of 3D trabecular microarchitecture are dependent of the rod / plate models such as the Structural Model Index (SMI) and morphological parameters derived from Mean Intercept Length (MIL) methods<sup>29</sup>. We have not used such parameters to assess the cortical parameters since cortical bone is not organized following this model of rod and plate. Then, we obtained three dimensional renderings of the porosity network and measurements of cortical parameters analogous to trabecular bone ones.

Only a few papers in the literature described cortical porosity characterization in three dimensions<sup>8,17,30</sup>. In the major part of these studies, authors reported the calculation of the global intracortical porosity (PoV/TV equivalent). As shown for example by Wachter et al.<sup>17</sup>, 3D intracortical porosity measured by  $\mu$ CT was significantly correlated with histological porosity and with some parameters such as osteon dimension and BMD. Our correlation between 2D and 3D porosity measurements was in the same order ( $r = 0.91$ ) than those found by Wachter et al ( $r = 0.95$ ,  $p < 10^{-4}$ ).

Wang et al.<sup>30</sup> reported a 3D approach by using low field pulsed Nuclear Magnetic Resonance (NMR). The validation has been performed by comparison with histological measurements. They calculated a determination coefficient for bone porosity ( $r^2 = 0.72$ ). Based on the NMR principle, they measured the relaxation time of fluid in the pores of cortical bone. This time is directly proportional to the surface to volume ratio. Assuming that Haversian canals are quasi-cylindrical, they deduced the diameters of the pores and the pore size distributions from this relaxation time. In our quantitative analysis, the calculation of the pore diameter was carried out without any model assumption. The distribution of pore diameter was obtained with 15  $\mu\text{m}$  interval. Literature reported that Havers and Volkmann canals have a diameter around 50  $\mu\text{m}$  for healthy bone<sup>31</sup> and much larger for osteoporotic bone<sup>30</sup>. They constitute the major part of the femoral cortical porosity while resorption cavities have been reported to be in the order of 200 to 300  $\mu\text{m}$ <sup>8</sup>. Porosity with diameter less than 20  $\mu\text{m}$  could be attributed either to lacunae<sup>30</sup> or smaller Haversian canals<sup>32</sup>.

To our knowledge, the first approach of  $\mu\text{CT}$  cortical bone porosity has been reported by Cooper et al.<sup>8</sup>. They carried out the calculations on two samples and discussed potentialities and limitations of the technique for the evaluation of the cortical canal network. The authors showed that one limitation of their study might be the resolution which could induce errors in quantitative parameters due to canal disconnections. Finally, they have demonstrated that improving the resolution to 5  $\mu\text{m}$  dramatically improved the 3D canal continuity.  $\mu\text{CT}$  with a resolution around 10 micrometers is commonly used for trabecular bone imaging. The best resolution is achieved with Synchrotron radiation (SR)  $\mu\text{CT}$ . Using this technique with a 1.4  $\mu\text{m}$  spatial resolution, Peyrin et al.<sup>33</sup> have evidenced osteocyte lacunae. In conventional  $\mu\text{CT}$  using a cone beam, the sample must be moved closer to the detector to improve the resolution, thus decreasing the volume of interest. Therefore, a

compromise has to be found between the spatial resolution and the volume to analyze. Thus, to determine the global intracortical porosity, a very good resolution (better than 10  $\mu\text{m}$ ) is not necessary. In Wachter et al's study<sup>17</sup>, the resolution was fixed at 30  $\mu\text{m}$  which allows measurement of the global porosity on a large volume of interest. The validation of the porosity measured by  $\mu\text{CT}$  was made by comparison with histological sections (100  $\mu\text{m}$  thick). They obtained a correlation coefficient  $r$  of 0.95 ( $p < 10^{-4}$ ). Nevertheless, a better resolution is necessary to analyze the cortical microstructure. Indeed in our experiment, when calculating the distribution of the pore size, up to 35 % of the pores (Femurs I level A and II level B) had diameter lower than 40  $\mu\text{m}$ .

The 3D renderings which were obtained from  $\mu\text{CT}$  sections allowed to observe the qualitative differences in the microstructure of the cortical network porosity (Fig. 5), where Volkman and Havers canals can be distinguished. The vertical canals are predominant leading to a high degree of cortical anisotropy. This value was found higher than in trabecular bone. Whitehouse<sup>34</sup> has found the maximal degree of anisotropy under 2.2 in trabecular bone while the values in the present study ranged from 1.97 to 3.26 (Table 1). We observed that the degree of anisotropy assessed by the MIL method was depending on pore size. This led to high DA in the specimen with high porosity. It is probably due to the fact that most of resorption lacunae preserved a preferential orientation in parallel to the surface of bone. In the trabecular bone, the anisotropy constituted an important determinant of the bone strength and should be considered to predict the fracture risk<sup>35</sup>. We have found in cortical bone a significant correlation between the degree of anisotropy and mechanical parameters, but this correlation was lower ( $r = 0.53$ ) than for the morphological parameters ( $0.74 < r < 0.94$ ) (Table 3). However, the Young modulus and the elastic coefficient were only assessed in the axial direction.

Similarly, the fractal dimension which could be a very interesting parameter in trabecular bone<sup>24,25</sup> has also a significant correlation with mechanical parameters in our study (Table 3). But this correlation ( $r = 0.75$ ) remains lower than for morphological parameters.

**In conclusion**, our 3D cortical porosity evaluation by  $\mu$ CT has been validated by the porosity measurement on SEM sections as we observed a strong relationship between 2D and 3D porosity. Furthermore, we have for the first time shown that the microarchitecture of cortical bone is related to the Young modulus and the elastic coefficient from ultrasound measurements. The calculation of the morphological and topological parameters by using algorithms usually devoted to trabecular bone analysis and independent of any model appear reliable to analyze the cortical bone structure. Many factors are implicated in the mechanical properties of bone : porosity, density, mineral content, collagen fibers orientation.... Therefore, in addition to porosity measurement, other microstructural parameters like spatial organization of porosity and size of pores are involved in bone mechanical strength. These results are of importance to improve the clinical assessment of bone quality. They might help clinicians and researchers to get a better understanding and evaluation of risk of fracture in elderly patients.

## REFERENCES

1. Hildebrand T, Laib A, Muller R, Dequeker J, Ruegsegger P. Direct three-dimensional morphometric analysis of human cancellous bone: microstructural data from spine, femur, iliac crest, and calcaneus. *J Bone Miner Res* 1999;14:1167-1174.
2. Dufresne TE, Chmielewski PA, Manhart MD, Johnson TD, Borah B. Risedronate preserves bone architecture in early postmenopausal women in 1 year as measured by three-dimensional microcomputed tomography. *Calcif Tissue Int* 2003;73:423-432.
3. Patel V, Issever AS, Burghardt A, Laib A, Ries M, Majumdar S. MicroCT evaluation of normal and osteoarthritic bone structure in human knee specimens. *J Orthop Res* 2003;21:6-13.
4. Kinney JH, Ladd AJ. The relationship between three-dimensional connectivity and the elastic properties of trabecular bone. *J Bone Miner Res* 1998;13:839-845.
5. van Rietbergen B, Odgaard A, Kabel J, Huiskes R. Relationships between bone morphology and bone elastic properties can be accurately quantified using high-resolution computer reconstructions. *J Orthop Res* 1998;16:23-28.
6. Mundy GR, Chen D, Oyajobi BO. Bone remodeling. In: Murray J. Favus, editor. *Primer on the metabolic bone diseases and disorders of mineral metabolism*. Washington: American Society for Bone and Mineral Research;2003. p. 46-58.
7. McCalden RW, McGeough JA, Barker MB, Court-Brown CM. Age-related changes in the tensile properties of cortical bone. The relative importance of changes in porosity, mineralization, and microstructure. *J Bone Joint Surg Am* 1993;75:1193-1205.
8. Cooper DM, Turinsky AL, Sensen CW, Hallgrímsson B. Quantitative 3D analysis of the canal network in cortical bone by micro-computed tomography. *Anat Rec* 2003;274:169-179.
9. Wachter NJ, Krischak GD, Mentzel M, Sarkar MR, Ebinger T, Kinzl L et al. Correlation of bone mineral density with strength and microstructural parameters of cortical bone in vitro. *Bone* 2002;31:90-95.
10. Dong XN, Guo XE. The dependence of transversely isotropic elasticity of human femoral cortical bone on porosity. *J Biomech* 2004;37:1281-1297.
11. Stein MS, Feik SA, Thomas CD, Clement JG, Wark JD. An automated analysis of intracortical porosity in human femoral bone across age. *J Bone Miner Res* 1999;14:624-632.
12. Bousson V, Meunier A, Bergot C, Vicaud E, Rocha MA, Morais MH et al. Distribution of intracortical porosity in human midfemoral cortex by age and gender. *J Bone Miner Res* 2001;16:1308-1317.
13. Laval-Jeantet AM, Bergot C, Carroll R, Garcia Schaefer F. Cortical bone senescence and mineral bone density of the humerus. *Calcif Tissue Int* 1983;35:268-272.

14. Brockstedt H, Kassem M, Eriksen EF, Mosekilde L, Melsen F. Age and sex related changes in iliac cortical bone mass and remodeling. *Bone* 1993;14:681-691.
15. Bousson V, Bergot C, Meunier A, Barbot F, Parlier-Cuau C, Laval-Jeantet AM et al. CT of the middiaphyseal femur : cortical bone mineral density and relation to porosity. *Radiology* 2000;217:179-187.
16. Cooper DM, Matyas JR, Katzenberg MA, Hallgrímsson B. Comparison of microcomputed tomographic and microradiographic measurements of cortical bone porosity. *Calcif Tissue Int* 2004;74:437-447.
17. Wachter NJ, Augat P, Krischak GD, Mentzel M, Kinzl L, Claes L. Prediction of cortical bone porosity in vitro by microcomputed tomography. *Calcif Tissue Int* 2001;68:38-42.
18. Stout SD, Brunnsden BS, Hildebolt CF, Commean PK, Smith KE, Tappen NC. Computer-assisted 3D reconstruction of serial sections of cortical bone to determine the 3D structure of osteons. *Calcif Tissue Int* 1999;65:280-284.
19. Bousson V, Peyrin F, Bergot C, Hausard M, Sautet A, Laredo JD. Cortical bone in the human femoral neck : three-dimensional appearance and porosity using synchrotron radiation. *J Bone Miner Res* 2004;19:794-801.
20. Bensamoun S, Gherbezza JM, de Belleval JF, Ho Ba Tho MC. Transmission scanning acoustic imaging of human cortical bone and relation with the microstructure. *Clin Biomech* 2004;19:639-647.
21. Hildebrand T, Ruegsegger P. A new method for the model independent assessment of thickness in three dimensional images. *J Microsc* 1997;185:67-75.
22. Ulrich D, Van Rietbergen B, Laib A, Ruegsegger P. The ability of three dimensional structural indices to reflect mechanical aspects of trabecular bone. *Bone* 1999;25: 55-60.
23. Harrigan TP, Mann RW. Characterization of microstructural anisotropy in orthotropic materials using a second rank tensor. *J Mater Sci* 1984;19:761-767.
24. Link TM, Majumdar S, Augat P, Lin JC, Newitt D, Lu Y et al. In vivo high resolution MRI of the calcaneus : differences in trabecular structure in osteoporosis patients. *J Bone Miner Res* 1998;13:1175-1182.
25. Mawatari T, Miura H, Higaki H, Moro-Oka T, Kurata K, Murakami T et al. Effect of vitamin K<sub>2</sub> on three dimensional trabecular microarchitecture in ovariectomized rats. *J Bone Miner Res* 2000;15:1810-1817.
26. Ho Ba Tho MC. SIP 305 © Inserm Logiciel de prétraitement d'images médicales Scanner et IRM;1993.
27. Ashman RB, Cowin SC, Van Buskirk WC, Rice JC. A continuous wave technique for the measurement of the elastic properties of cortical bone. *J Biomech* 1984;17:349-361.
28. Dieulesaint E, Royer D. Ondes élastiques dans les solides. Paris:Editions Masson ;1974.

29. Parfitt AM, Drezner MK, Glorieux FH, Kanis JA, Malluche H, Meunier PJ et al. Bone histomorphometry : standardization of nomenclature, symbols and units. *J Bone Miner Res* 1987;2:595-610.
30. Wang X, Ni Q. Determination of cortical bone porosity and pore size distribution using a low field pulsed NMR approach. *J Orthop Res* 2003;21:312-319.
31. Martin RB. Porosity and specific surface of bone. *Crit Rev Biomed Eng* 1984;3: 179-222.
32. Pfeiffer S. Variability in osteon size in recent human populations. *Am J Phys Anthropol* 1998;106:219-227.
33. Peyrin F, Salome M, Cloetens P, Laval-Jeantet AM, Ritman E and Rüegsegger P. Micro-CT examinations of trabecular bone samples at different resolutions : 14, 7 and 2 micron level. *Technol Health Care* 1998;6:391-401.
34. Whitehouse WJ. The quantitative morphology of anisotropic trabecular bone. *J Microsc* 1974;101:153-168.
35. Sugita H, Oka M, Toguchida J, Nakamura T, Ueo T, Hayami T. Anisotropy of osteoporotic cancellous bone. *Bone* 1999;24:513-516.

**Table 1 :** Average, standard deviation, minimal and maximal values of the morphological parameters measured with  $\mu$ CT for the three femurs versus the level on the femur.

	Proximal	Mid diaphysis	Distal	Distal
	FI	FII	FII	FIII
3D PoV/TV (%)	$3.8 \pm 3.1$ 0.93 – 6.45	$9.3 \pm 5.7$ 3.8 – 18.5	$51.3 \pm 7.70$ 42.3 – 63.1	$58.8 \pm 16.0$ 34.0 – 67.4
PoS/PoV ( $\text{mm}^{-1}$ )	$94 \pm 30$ 58 – 128	$53 \pm 25$ 18 – 79	$12 \pm 1$ 9 – 13	$13 \pm 4$ 9 – 19
PoDm ( $\mu\text{m}$ )	$58 \pm 16$ 45 – 79	$159 \pm 116$ 67 – 248	$426 \pm 56$ 359 – 493	$335 \pm 41$ 277 – 368
PoS <sub>p</sub> ( $\mu\text{m}$ )	$322 \pm 102$ 179 – 420	$312 \pm 53$ 250 – 393	$258 \pm 32$ 220 – 305	$208 \pm 32$ 161 – 229
PoN ( $\text{mm}^{-1}$ )	$0.60 \pm 0.42$ 0.25 – 1.10	$0.63 \pm 0.15$ 0.47 – 0.86	$1.22 \pm 0.25$ 0.86 – 1.44	$1.72 \pm 0.33$ 1.23 – 2.12
DA	$1.97 \pm 0.64$ 1.26 – 2.76	$2.29 \pm 0.50$ 1.79 – 3.05	$3.26 \pm 0.90$ 2.25 – 4.41	$2.81 \pm 0.60$ 2.56 – 3.84
FD	NA	$2.44 \pm 0.07$ 2.38 – 2.53	$2.88 \pm 0.08$ 2.80 – 2.96	$2.81 \pm 0.24$ 2.40 – 2.97

PoS pore surface, PoV pore volume, PoDm pore diameter, PoSp pore spacing, PoN pore number, DA degree of anisotropy, FD fractal dimension, NA non available.

**Table 2 :** Multiple regression for porosity using the combination of morphological parameters measured with  $\mu$ CT (PoV/TV) and SEM (porosity) techniques

Dependent variables	Independent variables	$r^2$	p
Porosity (PoV/TV)	PoN	0.80	$p < 10^{-4}$
	PoN, PoDm	0.96	$p < 10^{-4}$
(PoV/TV = 35.18 PoN + 0.11 PoDm - 42.0)			

**Table 3** : Spearman correlation coefficient (r values) between structural parameters and mechanical properties evaluated by ultrasound technique on the three femurs.

	PoV/TV	PoS/PoV	PoDm	PoS <sub>p</sub>	PoN	DA	FD
E <sub>33</sub>	-0.92 <sup>a</sup>	0.87 <sup>a</sup>	-0.77 <sup>b</sup>	0.74 <sup>b</sup>	-0.86 <sup>a</sup>	-0.54 <sup>b</sup>	0.76 <sup>b</sup>
C <sub>33</sub>	-0.94 <sup>a</sup>	0.90 <sup>a</sup>	-0.80 <sup>a</sup>	0.76 <sup>b</sup>	-0.88 <sup>a</sup>	-0.53 <sup>b</sup>	0.75 <sup>b</sup>

<sup>a</sup>p<10<sup>-4</sup>, <sup>b</sup>p<5.10<sup>-2</sup>

E<sub>33</sub> Young modulus (Pa), C<sub>33</sub> elastic coefficient (Pa)

## Figure Legends

Figure 1 : Anatomical localisation in the diaphysis of the samples on the three femurs.

Figure 2 : Histograms of reconstructed cortical bone samples of the femur II.

Figure 3 : Ultrasonic transmission technique in contact.

Figure 4 : Three dimensional visualization of sub region of two samples (cortical porosity 4.5 % for the top and 42.3 % for the bottom). (a) on a slice, the region of interest ( $1200 \times 1300 \mu\text{m}^2$ ) is defined. (b) the reconstruction was carried out through 200 slices, corresponding to 1.5mm. (c) is the negative image of (b) representing the network of porosity in the volume.

Figure 5 : 3D renderings of cortical porosity network in a sample from proximal diaphysis section (Femur I, global porosity 1.2 %) (dimension of the volume of interest for the reconstruction :  $1.4 \times 1.6 \times 2.3 \text{ mm}^3$ ).

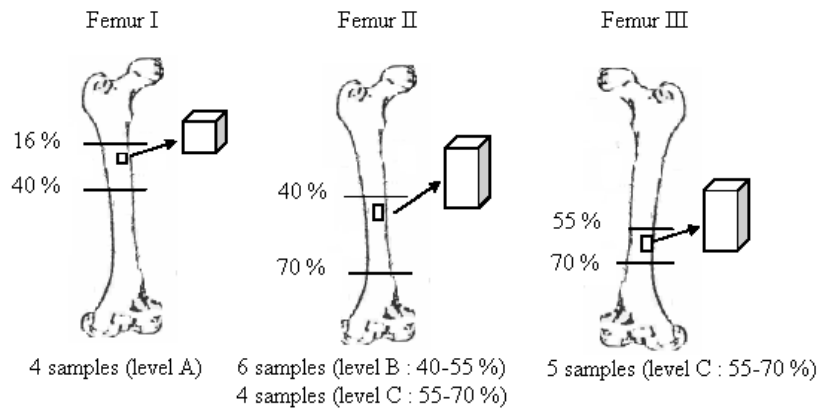


Figure 1 : Anatomical localisation in the diaphysis of the samples on the three femurs.

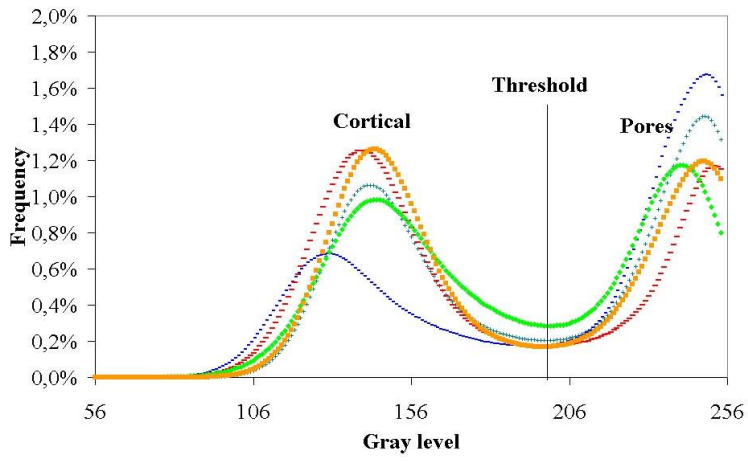


Figure 2 : Histograms of reconstructed cortical bone samples of the femur II.

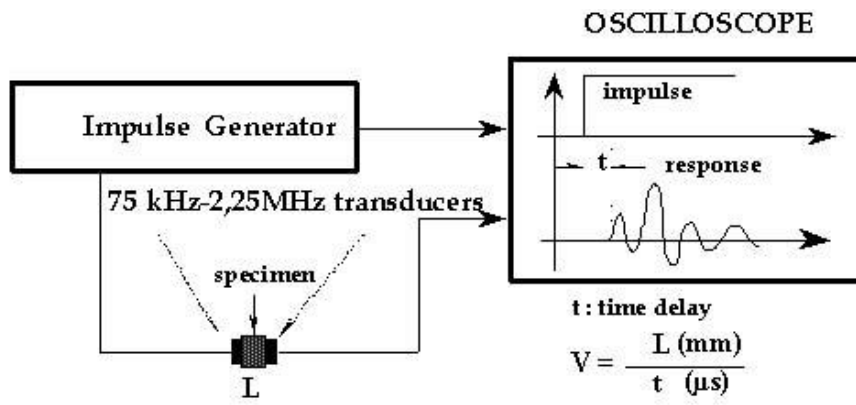


Figure 3 : Ultrasonic transmission technique in contact.

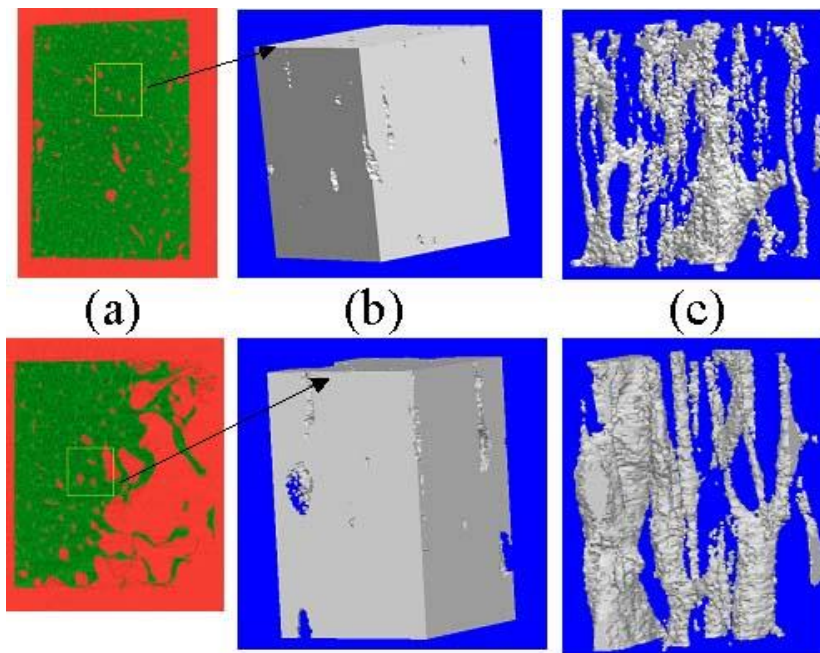


Figure 4 : Three dimensional visualization of sub region of two samples (cortical porosity 4.5 % for the top and 42.3 % for the bottom).

(a) On a slice, the region of interest ( $1200 \times 1300 \mu\text{m}^2$ ) is defined.

(b) The reconstruction was carried out through 200 slices, corresponding to 1.5mm.

(c) The negative image of (b) representing the network of porosity in the volume.

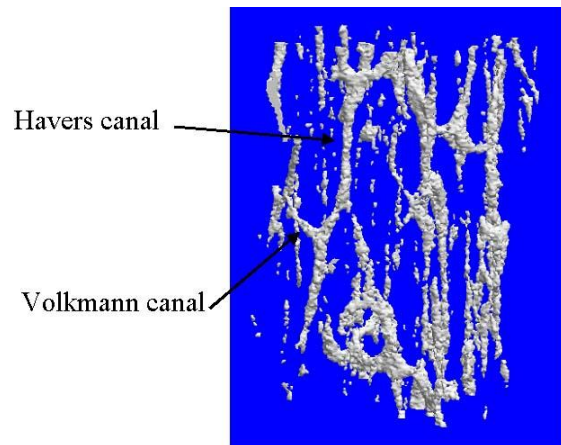


Figure 5 : Visualization 3D of cortical porosity network in a sample from high diaphysis section (Femur I, global porosity 1.2 %) (dimension of the volume of interest for the reconstruction :  $1.4*1.6*2.3 \text{ mm}^3$ ).

